Adv. Space Res. Vol. 13, No. 10, pp. (10)55–(10)64, 1993
Printed in Great Britain.

0273–1177/93 $24.00

FINITE ELEMENT SIMULATION (FES): A COMPUTER MODELING TECHNIQUE FOR STUDIES OF CHEMICAL MODIFICATION OF THE IONOSPHERE

M. Mendillo, J. Semeter and J. Noto

Center for Space Physics, Boston University, 725 Commonwealth Avenue, Boston, MA 02215, U.S.A.

Abstract

A numerical modeling code for ionospheric modification experiments has been developed using finite element simulation (FES) techniques. The FES approach to multi-component diffusion and chemistry is described in the context of chemical release "active experiments" in the F-region ionosphere. Comparisons of simulation results matched to cases for which analytical solutions exist, as well as with actual experimental observations, point to a successful and versatile capability for predicting and interpreting chemical induced ionospheric modifications.

Introduction

Finite element simulation (FES) is a computational technique used to model the diffusion and chemistry of neutral and charged species in a realistic multi-component atmosphere. It was developed as a tool for modeling chemical release experiments in the F-region of the ionosphere /1/. In such experiments, released molecules diffuse through an ambient atmosphere where they may react with ambient neutral and plasma species. Reactions with plasma species lead to observable ionospheric depletions and associated airglow generation due to rapid recombination of ions and electrons. Other applications include modeling of ambient ionospheric processes at mid-latitudes /2,3/ as well as meridional structure in the auroral and sub-auroral F-region /4/. In this report we expand our description of FES techniques and update all rate coefficients needed for active experiments that produce airglow enhancements.

The ionospheric phenomena of interest can be described in terms of the following equation:

$$\frac{\partial n_i}{\partial t} = \nabla \cdot [D_i(\mathbf{r},t)\nabla n_i + G_i(\mathbf{r},t)n_i] - \sum_j k_{ij}(T) n_i n_j \qquad (1)$$

where n_i is the concentration of the diffusing species, D_i is the diffusion coefficient for species i, G_i is the drift velocity in a gravitational field, and k_{ij} is the chemical reaction rate between species i and j at temperature T. This expression has no general analytical solution. In the finite element approach, each non-linearly coupled processes is treated independently. Thus, the effects of one process, whether it is transport or chemical, are calculated at a given time for each cell in a three dimensional spatial grid while all other processes are held stationary. The resulting change in a cell is then considered to be a superposition of these linear effects. Such an approach lends itself to serial computer algorithms and greatly enhances conceptualization of complex physical systems. The validity of such a linearization must be considered. More specifically, can one choose a time step and a spatial grid size such that the system behaves as a set of first order linear differential equations? This will be addressed through stability analysis, comparisons to analytical solutions and by analyzing asymptotic behavior of solutions.

Finite Element Simulation Algorithm

The effects observed during a neutral release experiment exhibit approximate azimuthal symmetry about the release point. For the three dimensional FES model, the appropriate cell geometry is one of concentric annuli as shown in Figure 1. For releases in the F-region of the ionosphere, the grid covers a region from 100 to 740 km in height and from 0 to 320 km in radius. There are no restrictions on cell dimensions, so smaller cells can be used where concentration gradients are largest (e.g., near the center or release point). Cell heights range from 20 km at low altitudes to 100 km near the topside of the ionosphere. Radial cell dimensions vary from 5 km to 150 km. The vertical axis is oriented normal to the Earth's surface and is located at the longitude and latitude of the release. Figure 2 shows a cross-section of the grid used for modeling the REDAIR-2 experiment to be discussed below.

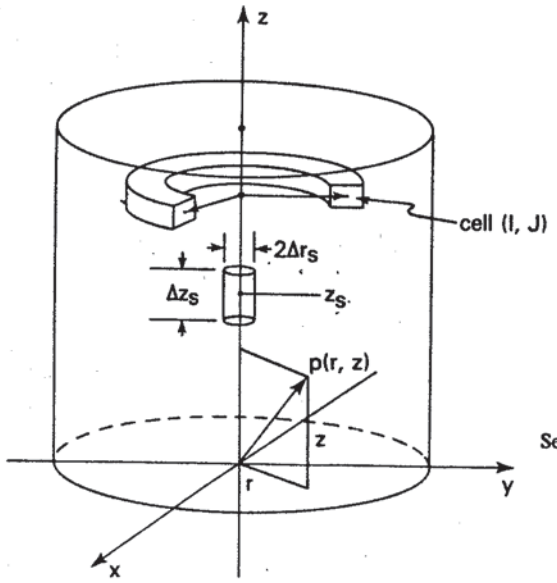

Figure 1: FES cell geometry used to make azimuthally symmetric spatial grid.

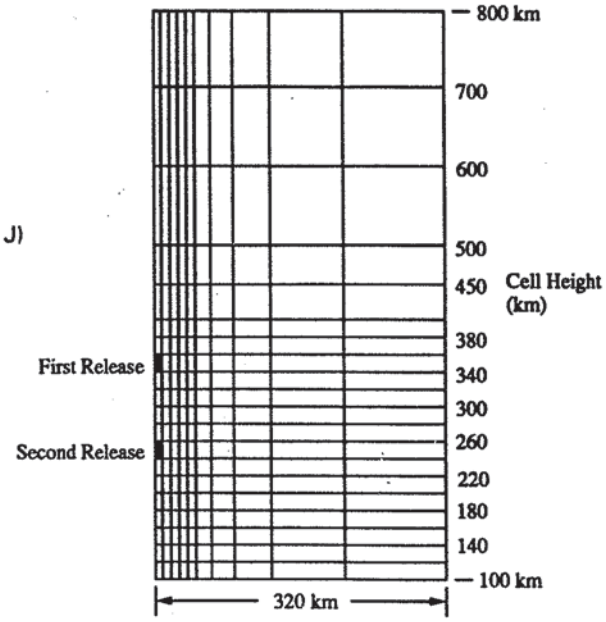

Figure 2: Cross section of spatial grid used to model REDAIR-2. Darkened cells indicate release points.

Transport

The net drift velocity in the vertical direction for ion species k, ignoring temperature driven drift /5/, is

$$U_k = D_k \left[\frac{1}{n_k} \frac{\partial n_k}{\partial z} + \frac{T_e}{T_i} \frac{1}{n_e} \frac{\partial n_e}{\partial z} + \frac{1}{H_k} \right] \tag{2}$$

where n_k is the number density of species k, n_e is the number density of electrons, T_e and T_i are the electron and ion temperatures and H_k is the scale height of species k. D_k is the net diffusion coefficient of species k through the background ions and neutrals calculated by /6,7/

$$\frac{1}{D_k} = \sum_{i \neq k} \frac{1}{D_{k,i}} \tag{3}$$

where $D_{k,i}$ is the diffusion coefficient of species k through species i. The summation does not include ions when k is a neutral due to their insignificant number density compared to the neutral background. However, ions must be included when the diffusing species, k, is an ion due to their strong Coulomb interaction.

Equation (2) can be made valid for neutral species by omitting the term involving n_e. For transport in the horizontal or x direction, the gravitational term D_k/H_k is omitted. For ion species, a further modification must be made. In the F-region of the Earth's ionosphere, the ion gyro frequency is much larger than the ion-neutral or ion-ion collision frequencies. This makes it possible to regard the plasma as being constrained to move only along magnetic field lines. Therefore, the drift velocity must be multiplied by $\sin^2 I$ for vertical [illegible]

Table 1: Diffusion Coefficients in FES. The table contains both release and ambient species. Ion species are only included in the second column when the diffusing species is an ion.

Species	D(cm^2/sec)
$O^+ \rightarrow O, O_2, N_2$	$\left[\frac{(T_i+T_n)^{.5}n(O)}{3.1\times10^{17}T_i} + \frac{n(O_2)}{7.2\times10^{15}T_i} + \frac{n(N_2)}{8.5\times10^{15}T_i}\right]^{-1}$
$O^+ \rightarrow OH^+, H_2O^+, O_2^+, NO^+$	$\frac{6.5\times10^7 T_i^{5/2}}{2.87n(OH^+)+2.91n(H_2O^+)+3.27n(O_2)+3.23n(NO^+)}$
$O_2^+ \rightarrow O, O_2, N_2$	$\left[\frac{(T_i+T_n)^{.5}n(O)}{1.7\times10^{16}T_i} + \frac{n(O_2)}{2.4\times10^{17}T_i} + \frac{n(N_2)}{1.1\times10^{16}T_i}\right]^{-1}$
$O_2^+ \rightarrow O^+, OH^+, H_2O^+, NO^+$	$\frac{6.5\times10^7 T_i^{5/2}}{3.33n(OH^+)+3.39n(H_2O^+)+3.27n(O)+3.93n(NO^+)}$
$NO^+ \rightarrow O, O_2, N_2$	$\frac{4.5\times10^{15}T_i}{n(N_2)+n(O_2)+n(O)}$
$NO^+ \rightarrow O^+, O_2^+, OH^+, H_2O^+$	$\frac{6.5\times10^7 T_i^{5/2}}{3.29n(OH^+)+3.35n(H_2O^+)+3.23n(O)+3.93n(O_2^+)}$
$OH^+ \rightarrow O, O_2, N_2$	$\frac{3.2\times10^{16}T_i}{2.55n(O)+4.2n(O_2)+4.31n(N_2)}$
$OH^+ \rightarrow O^+, O_2^+, H_2O^+, NO^+$	$\frac{6.5\times10^7 T_i^{5/2}}{2.87n(O^+)+3.33n(O_2^+)+2.96n(H_2O^+)+3.29n(NO^+)}$
$H_2O^+ \rightarrow O, O_2, N_2$	$\frac{3.2\times10^{16}T_i}{2.59n(O)+4.28n(O_2)+4.39n(N_2)}$
$H_2O^+ \rightarrow O^+, O_2^+, NO^+, OH^+$	$\frac{6.5\times10^7 T_i^{5/2}}{2.91n(O^+)+3.39n(O_2^+)+3.35n(NO^+)+2.96n(OH^+)}$
$SF_6 \rightarrow O, O_2, N_2$	$\frac{8.56\times10^{16}T_n^{.5}}{n(O)+n(O_2)+n(N_2)}$
$H_2 \rightarrow O, O_2, N_2$	$\left[\frac{n(O)}{2.97\times10^{18}T_n^{.5}} + \frac{n(O)}{2.8\times10^{17}T_n^{.74}} + \frac{n(O_2)}{3.06\times10^{17}T_n^{.732}}\right]^{-1}$
$N_2 \rightarrow O, O_2, N_2$	$\left[\frac{n(O)}{9.69\times10^{16}T_n^{.774}} + \frac{n(O_2)}{8.29\times10^{16}T_n^{.724}}\right]^{-1}$
$H_2O \rightarrow O, O_2, N_2$	$\left[\frac{n(O)}{8.46\times10^{17}T_n^{.5}} + \frac{n(N_2)}{2.04\times10^{17}T_n^{.632}} + \frac{n(O_2)}{2.02\times10^{17}T_n^{.632}}\right]^{-1}$
$CO_2 \rightarrow O, O_2, N_2$	$\left[\frac{n(O)}{5.87\times0^{17}T_n^{.5}} + \frac{n(N_2)}{6.58\times10^{16}T_n^{.752}} + \frac{n(O_2)}{5.77\times10^{16}T_n^{.749}}\right]^{-1}$
$O^* \rightarrow O, O_2, N_2$	$\left[\frac{n(O)}{5.37\times10^{17}T_n^{.5}} + \frac{n(N_2)}{4.76\times10^{17}T_n^{.5}} + \frac{n(O_2)}{6.58\times10^{17}T_n^{.5}}\right]^{-1}$

In some cases there may be more than one set of possible products for a reaction (such as the reaction of O_2^+ with an electron). So for generality, branching ratios, b_1 and b_2, are included to reflect the average number of a given product that will be created from the reaction (b_1 and b_2 are usually equal to 1). From equation (12), the new species concentrations are

$$\begin{aligned} n_A &= n_A - \Delta n_A \\ n_B &= n_B - \Delta n_B \\ n_C &= n_C + b_1 \Delta n_C \\ n_D &= n_D + b_2 \Delta n_D \end{aligned} \tag{13}$$

Table 2 lists the complete set of reaction rates used in FES. They reflect the current literature. Part A lists reactions occurring in the ambient atmosphere. Part B lists reactions related to chemical releases creating ionospheric holes and enhancing airglow.

Boundary Conditions

Care must be taken to establish appropriate boundary conditions in the FES model. Chemical processes pose no problem since they occur only within cells. Transport processes, however, could

Table 2: Reaction Rates Used in FES.

A. Ambient Chemistry in FES

Reaction	Rate	Reference
$O^+ + N_2 \longrightarrow NO^+ + N$	$2.78 \times 10^{-13} \exp[2.07(\frac{300}{T_i}) - 0.61(\frac{300}{T_i})^2]$	Chen et al. [1978]
$NO^+ + e^- \longrightarrow N + O$	$4.2 \times 10^{-7}(\frac{300}{T_e})^{0.85}$	Walls and Dunn [1974] Torr and Torr [1977] Alge et al. [1983]
$O^+ + O_2 \longrightarrow O_2^+ + O$	$3.23 \times 10^{-12} \exp[3.72(\frac{300}{T_i}) - 1.87(\frac{300}{T_i})^2]$	Chen et al. [1978]
$O_2^+ + e^- \longrightarrow O^* + O$	$1.95 \times 10^{-7}(\frac{300}{Te})^{0.7}$	Walls and Dunn [1974] Torr et al. [1976]
$O^* \longrightarrow O + 6300\text{Å}$	5.85×10^{-3}	Baluja and Zeippen [1988]
$O^* \longrightarrow O + photons$	7.7×10^{-3}	Baluja and Zeippen [1988]
$O^* + N_2 \longrightarrow O + N_2$	$2.0 \times 10^{-11} \exp[107.8/T_n]$	Streit [1976]
$O^* + e^- \longrightarrow O + e^-$	$8.1 \times 10^{-10}(\frac{T_e}{300})^{0.5}$	Link [1982]
$O^* + O_2 \longrightarrow O + O_2$	$2.9 \times 10^{-11} \exp[67.5/T_n]$	Streit [1976]
$O^* + O \longrightarrow O + O$	3.0×10^{-12}	Abreu et al. [1986] Yee et al. [1991]

B. Modification Chemistry in FES

Species Released	Reactions	Rates	References
CO_2	$CO_2 + O^+ \longrightarrow O_2^+ + CO$	9.4×10^{-10}	Hunton [1991]
	$O_2^+ + e^- \longrightarrow O^* + O$	$1.95 \times 10^{-7}(\frac{300}{T_e})^{0.7}$	Walls and Dunn [1974] Torr et al. [1976]
	$O^* + CO_2 \longrightarrow CO + CO$	$6.8 \times 10^{-11} \exp[\frac{117}{T_n}]$	Streit [1976]
H_2	$H_2 + O^+ \longrightarrow OH^+ + H$	1.7×10^{-9}	Bernhardt [1987]
	$OH^+ + e^- \longrightarrow O^* + H$	$7.5 \times 10^{-8}(\frac{300}{Te})^{0.5}$	Bernhardt [1987]
	$O^* + H_2 \longrightarrow OH + H$	$2.0 \times 10^{-11} \exp[\frac{107.8}{T_n}]$	Assumed Equal to $N_2 + O^*$
H_2O	$H_2O + O^+ \longrightarrow H_2O^+ + O$	3.2×10^{-9}	Bernhardt [1987]
	$H_2O^+ + e^- \longrightarrow OH^* + H$	$6.5 \times 10^{-7}(\frac{300}{Te})^{0.5}$	Bernhardt [1987]
	$O^* + H_2O \longrightarrow OH + OH$	2.3×10^{-10}	Streit [1976]
SF_6	$SF_6 + e^- \longrightarrow SF_5^- + F$	$\frac{2.2 \times 10^{-7}}{1 + 0.0016 \exp[4770/T_e]}$	Bernhardt [1987]

cause material to accumulate at boundary cells unless they are treated in a special way. At the bottomside of the F-region, transport is suppressed by the dense neutral atmosphere. For this reason, no special consideration needed to be made at the lower boundary. The boundary condition that has worked well at the topside and outermost cells is to prevent a change in concentration of any species to occur due to transport (chemistry is allowed). For this to work adequately, the spatial grid must contain enough cells so that concentration gradients remain small near the boundaries. Alternately, the boundary cells can be made very large, making transport times to these cells long in comparison to active experiment time scales ($\approx$ 20 minutes).

Spatial and Time Grids

The FES technique assumes there exists a domain over which the non-linearly coupled equations governing the dynamics of the ionosphere can be approximated in the linear way described above. Therefore, selection of spatial and temporal grids must be considered carefully. This is approached by first constraining the former. Regardless of the phenomenon under observation, the resolution of the observing technique defines the lower bound on the required cell size. Near the F-region peak, the resolution of optical and radar observations is greater than 10 km so there is no need for cell dimensions to be smaller. However, where spatial gradients under observation are small (e.g., horizontally, and near the topside of the F-region), cell sizes may be considerably larger.

With an appropriate spatial grid selected, an upper bound on Δt can be made from a stability argument. Consider one dimensional diffusion between two cells, i and $i+1$, as illustrated in Figure 3. If a concentration gradient exists, then diffusion can occur only until the concentrations are equal (i.e. diffusion is a first order process and no overshoot can occur). Therefore, in one Δt, the concentrations can at most equalize. If at t

$$n(i+1)\,|_t > n(i)\,|_t \tag{14}$$

then at $t+\Delta t$

$$n(i+1)\,|_{t+\Delta t} \geq n_i\,|_{t+\Delta t} \tag{15}$$

which can be written

$$n(i+1)\,|_t + \frac{\Delta N\,|_{\Delta t}}{V_{i+1}} \geq n(i)\,|_t - \frac{\Delta N\,|_{\Delta t}}{V_i} \tag{16}$$

For simplicity, assume $V_i = V_{i+1} = V$. Rearranging, it follows that

$$n(i+1)\,|_t - n(i)\,|_t \geq -2\frac{\Delta N\,|_{\Delta t}}{V} \tag{17}$$

Taking only the pressure term of Equation (7) and setting $I = 90^o$, equation (8) simplifies to

$$\Delta N = A\frac{D\Delta t}{\Delta x}\left[n(i+1)\,|_t - n(i)\,|_t\right] \tag{18}$$

Substituting (18) into (17) and setting $V = A \cdot \Delta x$ equation (17) simplifies to the expression

$$\Delta t \leq \frac{(\Delta x)^2}{2D} \tag{19}$$

which gives an upper bound for the choice of time grid. For a typical value of D and the smallest value for Δx, the time step is limited by $\Delta t \leq 2s$. This will guarantee a stable solution, but not necessarily an accurate one. To get a better idea of how small the time step must be, the asymptotic behavior of the model output must be examined for varying values of Δt.

Having a single time step for all processes wastes computer time, as quite often it is only a few processes which are proceeding quickly. The FES algorithm allows for each transport, chemical, and photo-chemical process to have its own time step. This is accomplished in the following manner. A maximum Δt is chosen using the stability criteria outlined above ($\sim 2s$). A table of possible time steps is then created from this value by successive divisions by 2 (i.e., 2, 1, .5, .25, etc.). In this manner, every larger Δt is an integer number of times greater than each time step below it. Initially, all processes (presently 30 in FES) are given the smallest time step. Each time a process is evaluated, the cell experiencing the maximum percentage change from that process is identified. If the percentage change is greater than 0.5%, the time step for that process is reduced to the next lower value in the table. If the change is less than 0.05%, the time step is increased, otherwise it remains the same. To maintain synchronization, a process is evaluated over and over until its own clock equals that of the master clock. The simulation then proceeds to the next process. After all processes are complete, the master clock advances to the next step in the overall time grid. The time step for the master clock is equal to the current largest process time step.

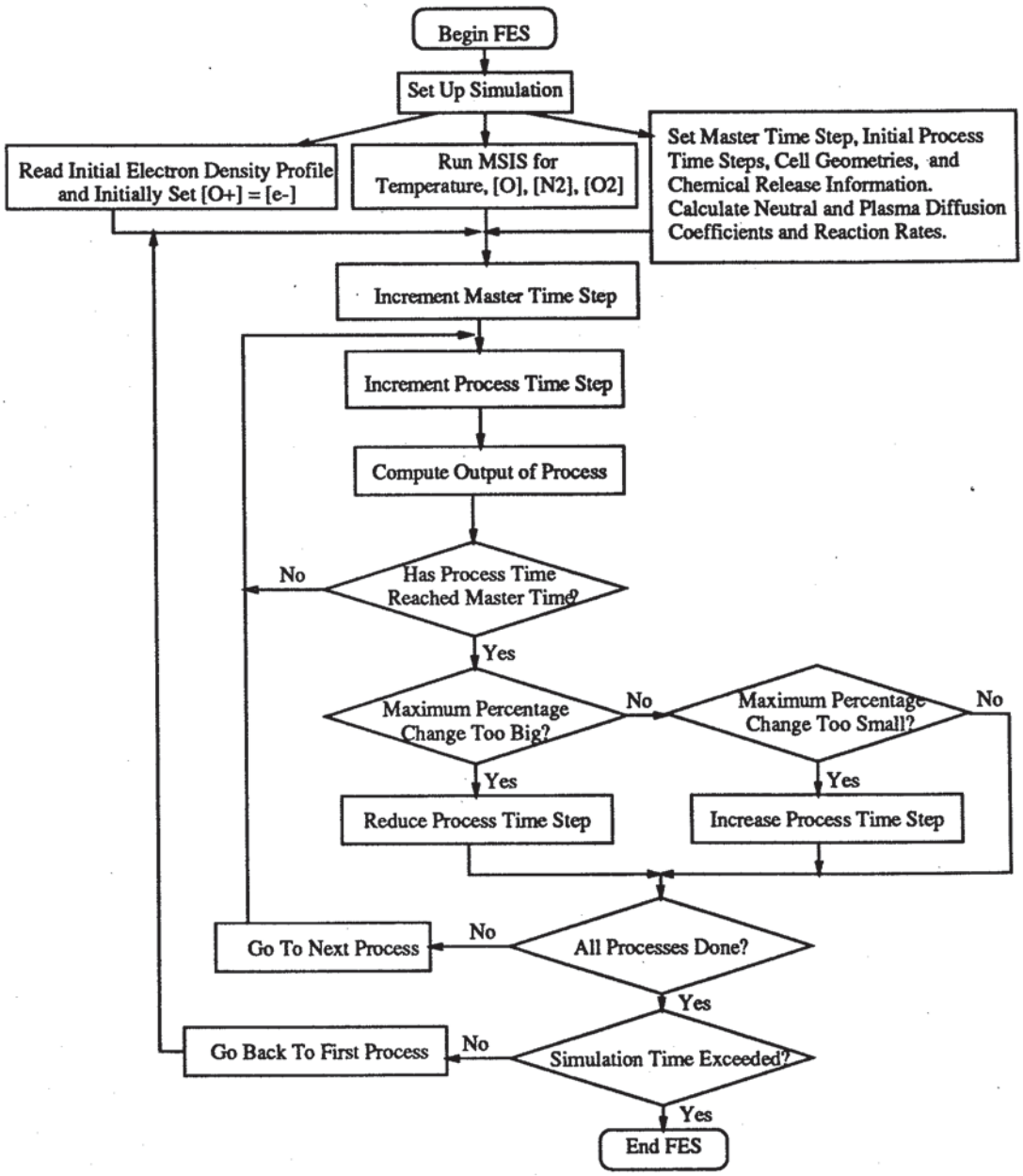

Figure 4: FES functional flow chart.

Program Outline

The FES program is outlined functionally in the flow diagram of Figure 4. The initial electron density and electron and ion temperature profiles for the release site are input to define the ionosphere. Since O^+ is the dominant F-region plasma species, n_{O+} is initially set equal to n_e. Neutral concentrations and temperatures (N_2, O_2, O, T_n) are calculated using the MSIS-86 model which requires the following inputs: year and day number, Universal Time, latitude and longitude, local solar time, 3 month average and daily average F10.7 flux, and the daily average magnetic index (A_p). All other species concentrations are initially set to zero. If T_e and T_i are not available, then $T_e = T_i \cong T_{msis}$ (a reasonable choice for post-sunset experiments). Additionally, FES requires the magnetic dip angle at the release point in order to calculate plasma diffusion. The user also sets up the spatial and initial temporal grids. All processes are set to the smallest time step as described in the previous section. In setting up the spatial grid, the cell location, density and release time of the modification species are also defined. Prior to beginning the simulation, FES calculates height/temperature dependent reaction rates. Diffusion coefficients are updated each time a process is called.

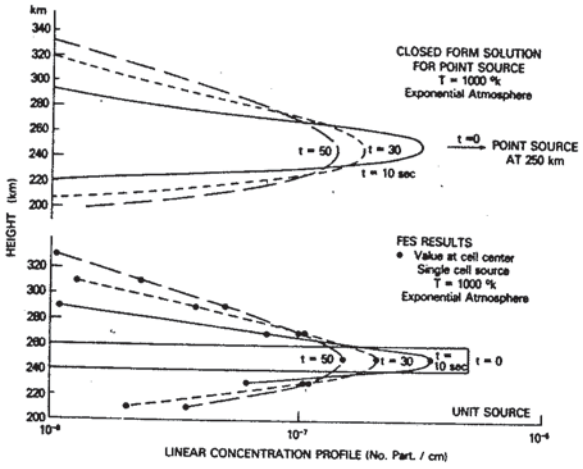

Figure 5: Comparison of analytical solution for diffusion with FES results.

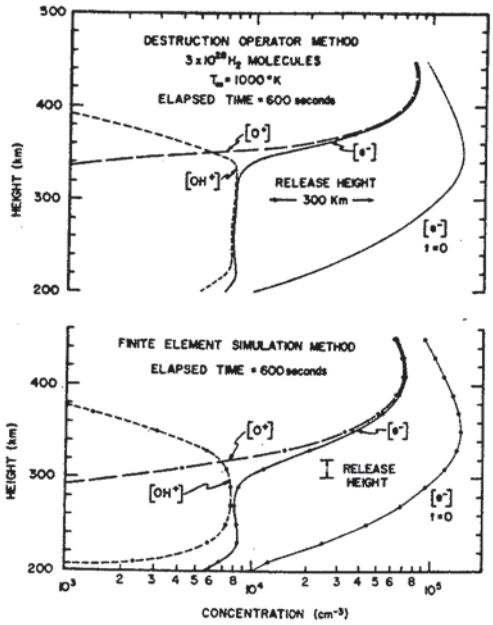

Figure 6: Comparison of FES results with analytical solution /24/.

Results

Model Verification

To test the FES model's numerical results against known analytical solutions, two types of case studies were configured. For diffusion under gravity of neutral gases released into an exponential atmosphere, closed form solutions exist /20,21/ that have been used for active experiment simulations /22,23,24/. A convenient way to check the inventory of diffusing particles is to integrate over radius and azimuth at a given height, thereby yielding linear concentration profiles (number of particles per cm of height). In Figure 5, results for a point source distribution show excellent agreement between the analytical and numerical methods. Similar consistencies were found for Gaussian source comparisons in which three FES source cells were used to approximate a distributed source.

To test coupled neutral diffusion and ionospheric depletion chemistry, model runs were conducted using the analytical "destruction operator" method /24/ and the FES code. As shown in Figure 6, there is excellent agreement between the F-region depletions computed by both methods. The small differences below 250 km result from the inclusion of multiple ion plasma diffusion in the FES approach that cannot be handled analytically. Figures 5 and 6 offer convincing evidence that the FES approach is well-suited to ionospheric simulation studies.

Simulation Results

To illustrate FES methods applied to a specific active experiment, Figures 7 and 8 give simulation results for the RED AIR-2 sounding rocket release of 40 lbs of CO_2 at two heights in the nighttime ionosphere above Wallops Island on 6 December 1991. While a detailed discussion of the photo-chemical processes and goals of the RED-AIR ("Release Experiments to Derive Airglow Inducing Reactions") program is beyond the scope of this paper, the observed $N_e(h)$ perturbations and associated 6300 Å airglow bursts were comparable to the predictions portrayed in Figures 7 and 8. The FES technique, as described above and tested successfully in Figures 5 to 8, provides an operational tool for predicting and post-mission modeling of a variety of chemical-release-induced active experiments in the mid-latitude F-region ionosphere.

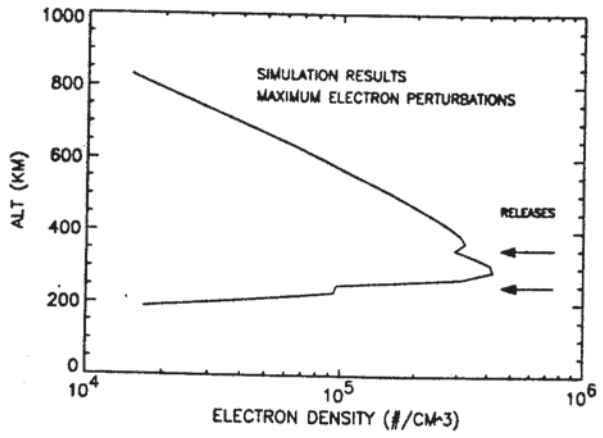

Figure 7: FES output for REDAIR-2 releases at 346 km and 248 km.

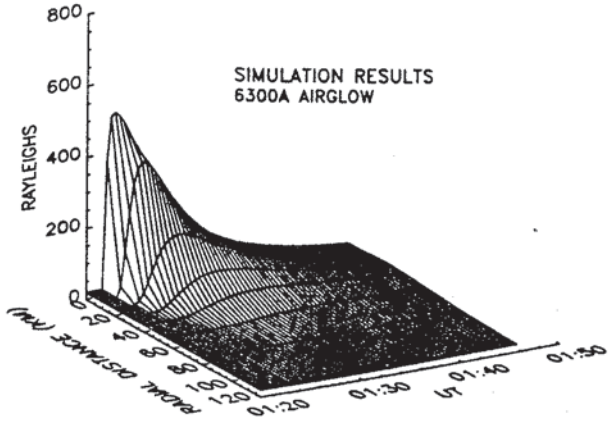

Figure 8: FES results for REDAIR-2 release at 248 km.

Acknowledgements

FES code development was supported by the NASA Spacelab-2 program, several AFGL contracts, the NASA CRRES program, by NASA grants NAG5-640 and NAS8-36324. We are deeply indebted to Dr. B. Balko's initial interest in this work and to the subsequent contributions made by Bradley Vance and Bruce Herniter.

References

1. Balko, B., and M. Mendillo, *Finite Element Simulation Applied to the Transport of Neutral and Ionized Particles in the Earth's Upper Atmosphere,* Astronomical Contributions Boston University Series III, No. 1, Boston, MA, 1977. see also
   Vance, B., and M. Mendillo, AFGL Tech. Rept #81-0119, Hanscom AFB 01731, April 1981.
2. Crary, D., and J. Forbes, *J. Geophys. Res.*, 91, 249, 1986.
3. Hagan, M., J. Forbes, and M. Codrescu, *Planet. Space Sci.*, 38, 1541, 1990.
4. Vance, B., and M. Mendillo, AFGL Tech. Rept. #79-003, Hanscom AFB 01731, January 1979.
5. Banks, P.M., and T.E. Holzer, *J. Geophys. Res.*, 74, 6305. 1979.
6. Hastings, J.T., and R.G. Roble, *Planet. Space Sci.*, 25, 209. 1977.
7. Banks, P.M., and G. Kockarts, *Aeronomy,* Academic Press, New York, 1973.

8. Rishbeth, H. and O. Garriott, *Introduction to Ionospheric Physics.* Academic Press, NY, 1969.
9. Chen, A., R. Johnsen, and M. A. Biondi, *J. Chem. Phys.*, *69*, 2688, 1978.
10. Walls, F.L., and G.H. Dunn, *J. Geophys. Res.*, 79, 1911, 1974.
11. Torr, M.R., and D.G. Torr, *Planet. Space Sci.*, 20, 91,1982.
12. Alge, E., N.G. Adams, and D. Smith, *J. Phys. B.*, 16, 1433, 1983.
13. Baluja, K.L., and C.J. Zeippen, *J. Phys. B.*, 21, 1455, 1988.
14. Streit, G.E., J.H. Carleton, A.L. Schmeltekopf, J.A. Davidson, and H.I. Schiff, *J. Chem. Phys.*, 65, 4716, 1976.
15. Link, R.,Ph.D. thesis, York Univ., Toronto, Canada, 1982.
16. Abreu, V.J., J.H. Yee, S.C. Solomon, and A. Dalgarno, *Planet Space Sci.*, 11, 1143, 1986.
17. Yee, J.H., S.L. Gruberman, and A.Dalgarno, *Planet. Space Sci.*, 38, 647, 1990.
18. Hunton, D.E., A.A. Viggiano, R.A. Morris, J.F. Paulson, D. Smith, and N.G. Adams, *J. Geophys. Res.*, 96, 13,881, 1991.
19. Bernhardt, P.A., *J. Geophys. Res.*, 92, 4617, 1987.
20. Yu, K., and M.M. Klein, *Phys. Fluids*, 7, 651, 1964.
21. Klein, M.M., and K. Yu, *J. Geophys. Res.*, 73, 1829, 1968.
22. Bernhardt, P.A., C.G. Park, and P.M. Banks, *Geophys. Res. Let.*, 2, 341, 1975.
23. Forbes, J.M., and M. Mendillo, *J. Atmos. Terr. Phys.*, 38, 1299, 1976.
24. Mendillo, M. and J.M. Forbes, *J. Geophys. Res.*, 83, 151, 1978.